ELSEVIER

Journal of the Mechanics and Physics of Solids
52 (2004) 1053–1069

JOURNAL OF THE MECHANICS AND PHYSICS OF SOLIDS

www.elsevier.com/locate/jmps

Bounds on the distribution of extreme values for the stress in composite materials

Robert Lipton*

Department of Mathematics, Louisiana State University, Baton Rouge, LA 70803, USA

Received 27 November 2002; received in revised form 20 August 2003; accepted 20 September 2003

Abstract

Suitable macroscopic quantities beyond effective elastic properties are used to assess the distribution of stress within a composite. The composite is composed of N anisotropic linearly elastic materials and the length scale of the microstructure relative to the loading is denoted by ε. The stress distribution function inside the composite $\lambda^{\varepsilon}(t)$ gives the volume of the set where the norm of the stress exceeds the value t. The analysis focuses on the case when $0 < \varepsilon \ll 1$. A rigorous upper bound on $\lim_{\varepsilon \to 0} \lambda^{\varepsilon}(t)$ is found. The bound is given in terms of a macroscopic quantity called the macro stress modulation function. It is used to provide a rigorous assessment of the volume of over stressed regions near stress concentrators generated by reentrant corners or by an abrupt change of boundary loading.
© 2003 Elsevier Ltd. All rights reserved.

Keywords: A. Composite materials; B. Failure criteria; C. Stress concentrations

1. Introduction

In many cases, the initiation of failure in a composite specimen can be related to the elastic stress field present at the time of initiation, see Kelly and Macmillan (1986). Motivated by this, we examine the distribution of extreme values for the stress in the linear elastic regime. The focus here is to assess the size and location of the region over which the magnitude of the stress (or equivalent stress) exceeds a nominal value t. This approach is consistent with failure initiation criteria given by a critical equivalent stress t_c above which the composite is assumed to fail, see Jeulin (1994).

Composites made from N anisotropic linearly elastic materials are considered. The domain containing the composite is denoted by Ω and the stress tensor in the composite

* Tel.: +1-2255-781569; fax: +1-2255-784276.
E-mail address: lipton@math.lsu.edu (R. Lipton).

0022-5096/$ - see front matter © 2003 Elsevier Ltd. All rights reserved.
doi:10.1016/j.jmps.2003.09.033

at the point $\mathbf{x}$ is denoted by $\sigma^\varepsilon(\mathbf{x})$. Here ε gives the scale of the microstructure relative to the characteristic length scale of the loading and the dimensions of the composite specimen. Coordinate invariant measures of the stress are used in the formulation of failure criteria. In this treatment, we consider the equivalent stress given by

$$\sigma^\varepsilon_{\text{eq}} = \sqrt{\Pi(\sigma^\varepsilon)}, \quad \Pi(\sigma^\varepsilon) = \boldsymbol{\Pi}\sigma^\varepsilon : \sigma^\varepsilon, \tag{1.1}$$

where $\boldsymbol{\Pi}$ is a positive-definite fourth-rank tensor, see Tsai and Hahn (1980). Examples of (1.1) include the Von Mises equivalent stress given by

$$\begin{aligned}&((1/2)[(\sigma^\varepsilon_{11}-\sigma^\varepsilon_{22})^2+(\sigma^\varepsilon_{22}-\sigma^\varepsilon_{33})^2+(\sigma^\varepsilon_{11}-\sigma^\varepsilon_{33})^2]\\&\quad+3((\sigma^\varepsilon_{12})^2+(\sigma^\varepsilon_{13})^2+(\sigma^\varepsilon_{23})^2))^{1/2},\end{aligned} \tag{1.2}$$

and the magnitude of the stress given by $|\sigma^\varepsilon| = \sqrt{\sum_{ij=1}^3 (\sigma^\varepsilon_{ij})^2}$. The subset of the specimen where $\sigma^\varepsilon_{\text{eq}}$ exceeds the value $t>0$ is denoted by S^ε_t. The stress distribution function $\lambda^\varepsilon(t)$ gives the volume of the overstressed zone S^ε_t. One also defines the stress distribution inside each elastic phase. The volume of the set in the ith phase where $\sigma^\varepsilon_{\text{eq}}$ exceeds the value $t>0$ is denoted by $\lambda^\varepsilon_i(t)$.

In this work rigorous bounds on $\lambda^\varepsilon(t)$ and $\lambda^\varepsilon_i(t)$ are obtained in the limit of vanishing ε, see Propositions 1.1 and 1.2 of this section. These are used to provide rigorous asymptotic upper bounds on the volume of the over stressed regions near stress concentrators generated by reentrant corners or by an abrupt change of boundary loading. They provide estimates for the volume of the overstressed zones for sufficiently small ε. This is illustrated in Section 2 where three examples are given for fiber-reinforced shafts subject to anti-plane shear and torsion loading. Motivated by these examples general conditions are identified in Section 3 for which $\lim_{\varepsilon_k\to 0}\lambda^{\varepsilon_k}_i(t)$ exhibits polynomial or exponential decay with t. Lastly, we point out the recent work of Luciano and Willis (2003) where the boundary layer behavior of the stress and strain fields with respect to ε is investigated for random composite materials.

The bounds on $\lim_{\varepsilon\to 0}\lambda^\varepsilon(t,)$ and $\lim_{\varepsilon\to 0}\lambda^\varepsilon_i(t)$ are given in terms of the macro stress modulation functions. To introduce the macro stress modulation functions we consider a composite contained in the unit cube Q. The local elastic tensor for N anisotropic elastic materials is denoted by $\mathbf{C}(\mathbf{y})$. Each phase has an elastic tensor specified by $\mathbf{A}_i$ and $\mathbf{C}(\mathbf{y})=\mathbf{A}_i$ in the ith phase. The characteristic function of the ith phase is written as $\chi_i(\mathbf{y})$ and takes the value 1 in the ith phase and 0 otherwise. No constraint is placed on the arrangement of the phases inside Q. We construct an infinite periodic medium by repeated replication of the unit cube. For this case the strain $\epsilon(\mathbf{y})$ in the composite can be decomposed into a prescribed average strain $\bar{\varepsilon}$ and a Q periodic fluctuation $\varepsilon(\mathbf{w}(\mathbf{y}))$ where the periodic displacement $\mathbf{w}$ is the solution of

$$-\operatorname{div}\,(\mathbf{C}(\mathbf{y})(\epsilon(\mathbf{w}(\mathbf{y}))+\bar{\epsilon}))=0. \tag{1.3}$$

The stress in the composite is $\sigma(\mathbf{y})=\mathbf{C}(\mathbf{y})(\epsilon(\mathbf{w}(\mathbf{y}))+\bar{\epsilon})$. The average stress is related to the average strain $\bar{\epsilon}$ by $\bar{\sigma}=\mathbf{C}^{\text{E}}\bar{\epsilon}$, where $\mathbf{C}^{\text{E}}$ is the effective elastic tensor, see Milton (2002).

One is interested in the maximum equivalent stress in the ith phase generated by subjecting Q to the average or macroscopic stress $\bar{\sigma}$. With this in mind we introduce the macro stress modulation function. Set

$$f^i(\mathbf{S}^{\mathrm{E}}\bar{\sigma}) = \|\chi_i(\mathbf{y})\sigma_{\mathrm{eq}}(\mathbf{y})\|_{L^\infty(Q)}, \tag{1.4}$$

where $\mathbf{S}^{\mathrm{E}}$ is the effective compliance $(\mathbf{C}^{\mathrm{E}})^{-1}$. Here $\|\cdot\|_{L^\infty(Q)}$ denotes the L^∞ norm over the unit period cell Q. The macro stress modulation function $f^i(\mathbf{S}^{\mathrm{E}}\bar{\sigma})$ measures the amplification or diminution of $\bar{\sigma}$ by the microstructure.

It is easily seen that stress state is self similar under a rescaling of the configuration. Indeed, set $\varepsilon_k = 1/k$ and rescale the material properties by $\mathbf{C}^{\varepsilon_k}(\mathbf{y}) = \mathbf{C}(\mathbf{y}/\varepsilon_k)$. It is easily checked that the stress also rescales as $\sigma^{\varepsilon_k}(\mathbf{y}) = \sigma(\mathbf{y}/\varepsilon_k)$. Thus, the stress analysis for the ε_k scale microstructure reduces to the stress analysis for the un-rescaled configuration on the unit cube Q. However, in general the loading is not uniform and the specimen shape is incommensurate with a rescaled periodic replication of a configuration specified on the unit cube. Because of this, the stress state in the composite is not obtained directly through an analysis of the stress in the unit cube. In this paper a suitable multiscale analysis using macro stress modulation functions is shown to provide rigorous bounds on the volume of the overstressed zones $\lambda^\varepsilon(t)$ and $\lambda_i^\varepsilon(t)$ in the limit of vanishing ε.

The general boundary value problem for the specimen is given. The $\varepsilon_k = 1/k$ periodic composite inside the specimen is described by $\mathbf{C}^{\varepsilon_k}(\mathbf{x}) = \mathbf{C}(\mathbf{x}/\varepsilon_k)$. The specimen Ω is subjected to a body load $\mathbf{f}$. A traction $\mathbf{g}$ is applied to part of the boundary of the specimen and a displacement $\mathbf{u}^{\varepsilon_k} = \mathbf{U}_0$ is prescribed on the remaining part of the boundary. Here the body loads, boundary tractions and boundary displacements can be nonuniform. The stress and displacement in the specimen are denoted by σ^{ε_k} and $\mathbf{u}^{\varepsilon_k}$, respectively. The equation of elastic equilibrium is given by

$$-\operatorname{div}\sigma^{\varepsilon_k} = \mathbf{f}. \tag{1.5}$$

The elastic strain $\epsilon(\mathbf{u}^{\varepsilon_k})$ is related to the stress by $\sigma^{\varepsilon_k} = \mathbf{C}^{\varepsilon_k}\epsilon(\mathbf{u}^{\varepsilon_k})$.

The multiscale analysis proceeds in two steps. The first step is the homogenization step where the macroscopic stress is determined. From the theory of periodic homogenization (Bensoussan et al., 1978) σ^{ε_k} and $\epsilon(\mathbf{u}^{\varepsilon_k})$ converge to the macroscopic stress σ^{M} and strain $\epsilon(\mathbf{u}^{\mathrm{M}})$ as ε_k goes to zero. The macroscopic stress satisfies $\sigma^{\mathrm{M}}\mathbf{n} = \mathbf{g}$ on the part of the boundary experiencing traction and the macroscopic displacement $\mathbf{u}^{\mathrm{M}}$ satisfies $\mathbf{u}^{\mathrm{M}} = \mathbf{U}_0$ on the remaining part of the boundary. The macroscopic stress satisfies the equilibrium equation $-\operatorname{div}\sigma^{\mathrm{M}} = \mathbf{f}$. The stress and strain are related through the homogenized constitutive law

$$\sigma^{\mathrm{M}}(\mathbf{x}) = \mathbf{C}^{\mathrm{E}}\epsilon(\mathbf{u}^{\mathrm{M}}(\mathbf{x})). \tag{1.6}$$

The second step is a down-scaling step and gives the interaction between the macroscopic stress $\sigma^{\mathrm{M}}(\mathbf{x})$ and the microstructure. For each $\mathbf{x}$ one has the macroscopic strain $\epsilon^{\mathrm{M}}(\mathbf{x}) = \epsilon(\mathbf{u}^{\mathrm{M}}(\mathbf{x})) = \mathbf{S}^{\mathrm{E}}\sigma^{\mathrm{M}}(\mathbf{x})$ and one computes the microscopic response given by $\sigma(\mathbf{x},\mathbf{y}) = \mathbf{C}(\mathbf{y})(\epsilon(\mathbf{w}(\mathbf{x},\mathbf{y})) + \epsilon^{\mathrm{M}}(\mathbf{x}))$. For each $\mathbf{x}$ the Q periodic displacement $\mathbf{w}(\mathbf{x},\mathbf{y})$ solves

$$-\operatorname{div}_{\mathbf{y}}(\mathbf{C}(\mathbf{y})(\epsilon_{\mathbf{y}}(\mathbf{w}(\mathbf{x},\mathbf{y})) + \epsilon^{\mathrm{M}}(\mathbf{x}))) = 0, \ \mathbf{y} \text{ in } Q. \tag{1.7}$$

Here all derivatives with respect to the microscopic variable $\mathbf{y}$ are denoted with subscripts and $\mathbf{x}$ appears as a parameter. The relevant interaction is described by the macrostress modulation function $f^i(\mathbf{S}^E\sigma^M(\mathbf{x}))$ given by

$$f^i(\mathbf{S}^E\sigma^M(\mathbf{x})) = \|\chi_i(\mathbf{y})\sigma_{eq}(\mathbf{x},\mathbf{y})\|_{L^\infty(Q)}. \tag{1.8}$$

The set of points where $f^i(\mathbf{S}^E\sigma^M(\mathbf{x})) \geqslant t$ is denoted by $\{f^i(\mathbf{S}^E\sigma^M(\mathbf{x})) \geqslant t\}$. The volume of this set is denoted by $|\{f^i(\mathbf{S}^E\sigma^M(\mathbf{x})) \geqslant t\}|$.

The bound on the volume of the overstressed zone in the ith phase is given by

Proposition 1.1.

$$\lim_{\varepsilon_k\to 0}\lambda_i^{\varepsilon_k}(t) \leqslant |\{f^i(\mathbf{S}^E\sigma^M(\mathbf{x})) \geqslant t\}|. \tag{1.9}$$

We introduce the maximum

$$M(\mathbf{S}^E\sigma^M(\mathbf{x})) = \max_{i=1,\ldots,N} f^i(\mathbf{S}^E\sigma^M(\mathbf{x})) \tag{1.10}$$

and the set of points where $M(\mathbf{S}^E\sigma^M(\mathbf{x})) \geqslant t$ is denoted by $\{M(\mathbf{S}^E\sigma^M(\mathbf{x})) \geqslant t\}$. The volume of this set is denoted by $|\{M(\mathbf{S}^E\sigma^M(\mathbf{x})) \geqslant t\}|$. The bound on the volume of the overstressed zone in the specimen is given by

Proposition 1.2.

$$\lim_{\varepsilon_k\to 0}\lambda^{\varepsilon_k}(t) \leqslant |\{M(\mathbf{S}^E\sigma^M(\mathbf{x})) \geqslant t\}|. \tag{1.11}$$

Next consider a subdomain S of the composite specimen. The volume of the set of points in the ith elastic phase contained in S for which $\sigma^\varepsilon_{eq}(\mathbf{x}) > t$ is denoted by $\lambda_i^{\varepsilon_k}(t,S)$. The following propositions provide information on the location of overstressed zones.

Proposition 1.3. *If $f^i(\mathbf{S}^E\sigma^M(\mathbf{x})) < t$ for every point in S then*

$$\lim_{\varepsilon_k\to 0}\lambda_i^{\varepsilon_k}(t,S) = 0. \tag{1.12}$$

Similarly, the volume of the set of points in S for which $\sigma^\varepsilon_{eq}(\mathbf{x}) > t$ is denoted by $\lambda^{\varepsilon_k}(t,S)$. One has the following proposition given by

Proposition 1.4. *If $M(\mathbf{S}^E\sigma^M(\mathbf{x})) < t$ for every point in S then*

$$\lim_{\varepsilon_k\to 0}\lambda^{\varepsilon_k}(t,S) = 0. \tag{1.13}$$

Propositions (1.3) and (1.4) were derived in Lipton (2003).

Propositions 1.1–1.4 are employed to estimate the size and location of overstressed zones in composites. This is illustrated in Section 2 where examples are given. General conditions are identified in Section 3 for which $\lim_{\varepsilon_k\to 0}\lambda_i^{\varepsilon_k}(t,S)$ exhibit polynomial or exponential decay with t. It is shown in Section 4 that Propositions 1.1 and 1.2 are direct consequences of homogenization constraints relating the macrostress modulation

functions to the distribution of states for the equivalent stress. These constraints are introduced and proved in Lipton (2003). In that work the constraints are derived for the more general case of graded locally periodic microstructures and in the context of G convergence. Because of this the arguments given here deliver results identical to Propositions 1.1 and 1.2 for more general classes of composites described by continuously graded locally periodic microstructures and for G convergent sequences of elastic tensors, see Lipton (2003). Propositions 3.1–3.3 are derived in Section 5.

2. Upper bounds on overstressed regions

In this section we consider prismatic shafts reinforced with long cylindrical fibers with circular cross section. In the first example the shaft cross section has a reentrant corner, see Fig. 1. The angular width of the reentrant corner is $2\pi - \omega$ where $\pi < \omega < 2\pi$. The fiber microgeometry is periodic and the length scale of the period is $\varepsilon_k = 1/k$, see Fig. 2. In order to illustrate the stress assessment methodology we first

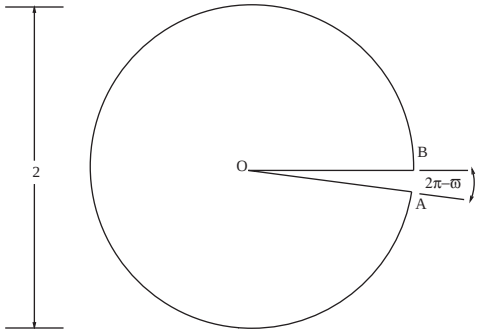

Fig. 1. Cross section of a long prismatic shaft with reentrant corner.

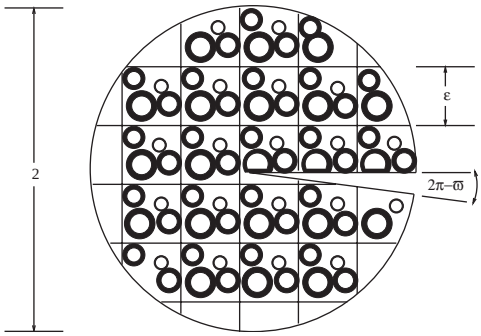

Fig. 2. The same shaft reinforced with long cylindrical fibers with circular cross section. The microstructure is periodic.

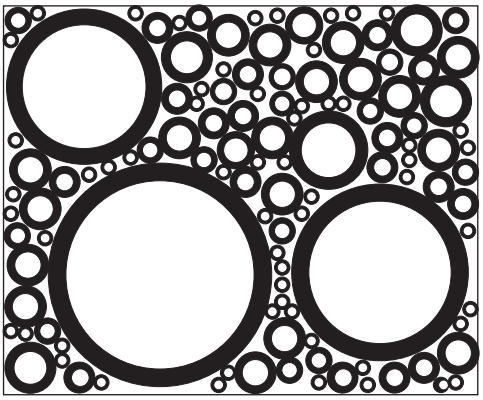

Fig. 3. The unit period cell for the microstructure. Here the unit cell is filled with the Hashin–Shtrikman-coated cylinder assemblage.

consider a period cell filled with microstructure for which the microstress and strain fields can be solved for analytically. Here we consider the coated cylinder assemblage of Hashin and Shtrikman (1962). A unit period cell filled with the coated cylinder assemblage is illustrated in Fig. 3. The coated cylinder assemblage is constructed by placing a space filling configuration of disks of different sizes ranging down to the infinitesimal inside the period cell. Each disk is partitioned in to a coating and a core. The area fractions of coating and core are the same for all disks. The matrix phase is given by the union of all the coatings and the fiber cross sections are given by the cores. The shear moduli of the fibers and matrix are denoted by $G_{\rm f}$ and $G_{\rm m}$ respectively. The area fraction of the fiber phase in the cross section is denoted by θ. The shaft is subject to anti-plane shear loading at the boundary. The out-of-plane deformation is denoted by u^{ε_k} and the associated out-of-plane stress components are given by the vector $\sigma^{\varepsilon_k}=(\sigma_1^{\varepsilon_k},\sigma_2^{\varepsilon_k})$. The rapidly oscillating piecewise constant shear stress is denoted by G^{ε_k} and $\sigma^{\varepsilon_k}=2G^{\varepsilon_k}\nabla u^{\varepsilon_k}$. The unit normal to the shaft cross section is denoted by $\mathbf{n}$. On $\overline{OA}$ and $\overline{OB}$ the shaft is traction free, i.e., $\sigma^{\varepsilon_k}\cdot\mathbf{n}=0$. On the circular arc of radius one connecting B to A the traction is given by $\sigma^{\varepsilon_k}\cdot\mathbf{n}=(\pi/\omega)\cos\phi\pi/\omega$, for $0<\phi<\omega$. Inside the shaft one has the equilibrium equations

$$2G_{\rm m}\Delta u^{\varepsilon_k}=0,\ \text{in the matrix and}$$

$$2G_{\rm f}\Delta u^{\varepsilon_k}=0,\ \text{in the fibers.} \tag{2.1}$$

The displacement is continuous across material interfaces and

$$2G_{\rm m}\partial_{\rm n}u_{\rm m}^{\varepsilon_k}=2G_{\rm f}\partial_{\rm n}u_{\rm f}^{\varepsilon_k}, \tag{2.2}$$

where $\partial_{\rm n}$ denoted the directional derivative along the unit normal pointing out of the fiber phase and the subscripts denote the side of the interface where the normal derivatives are evaluated.

In this example, we use Propositions 1.1–1.4 to provide rigorous upper bounds on the size of overstressed regions as well as a methodology for the assessment of their location in the reinforced cross section. The set in the fiber phase where $|\sigma^{\epsilon_k}| > t$ is denoted by $S^{\varepsilon_k}_{\mathrm{f},t}$ and the set in the matrix phase where $|\sigma^{\epsilon_k}| > t$ is denoted by $S^{\varepsilon_k}_{\mathrm{m},t}$. The areas occupied by the sets $S^{\varepsilon_k}_{\mathrm{f},t}$ and $S^{\varepsilon_k}_{\mathrm{m},t}$ are denoted by $\lambda^{\varepsilon_k}_{\mathrm{f}}(t)$ and $\lambda^{\varepsilon_k}_{\mathrm{m}}(t)$, respectively. The set where $|\sigma^{\epsilon_k}| > t$ in the composite is denoted by $S^{\varepsilon_k}_{t}$ and the area of this set is denoted by $\lambda(t)^{\varepsilon_k}$. In the sequel, we will also use the following standard convention: for a given function g we will denote the set of points for which the inequality $g(\mathbf{x}) \geqslant t$ holds by writing $\{g(\mathbf{x}) \geqslant t\}$. The volume of the set $\{g(\mathbf{x}) \geqslant t\}$ is denoted by $|\{g(\mathbf{x}) \geqslant t\}|$.

In order to compute the macrostress modulation functions we perform the multiscale analysis outlined in the introduction. The first step is the homogenization step. Passing to the limit as ε_k tends to zero the homogenization theory shows that the macroscopic out-of-plane displacement u^{M} and stress σ^{M} satisfy $\sigma^{\mathrm{M}} = 2G^{\mathrm{E}}\nabla u^{\mathrm{M}}$, where G^{E} is the effective shear stiffness for the coated cylinder assemblage given by

$$2G^{\mathrm{E}} = \beta\left(\frac{\beta(1-\theta)+\alpha(1+\theta)}{\beta(1+\theta)+\alpha(1-\theta)}\right). \tag{2.3}$$

Here $\beta = 2G_{\mathrm{m}}$ and $\alpha = 2G_{\mathrm{f}}$. One has $\nabla\cdot\sigma^{\mathrm{M}} = 0$ inside the shaft cross section. On the faces $\overline{OA}$ and $\overline{OB}$ traction free boundary conditions $\sigma^{\mathrm{M}}\cdot\mathbf{n} = 0$ are given. On the circular arc of radius one connecting B to A the traction is given by $\sigma^{\mathrm{M}}\cdot\mathbf{n} = (\pi/\omega)\cos\phi\pi/\omega$, for $0 < \phi < \omega$. The solution of the macroscopic problem gives

$$\sigma^{\mathrm{M}} = \mathbf{e}_r\frac{\pi}{\omega}r^{\pi/\omega-1}\cos\phi\pi/\omega - \mathbf{e}_\phi\frac{\pi}{\omega}r^{\pi/\omega-1}\sin\phi\pi/\omega. \tag{2.4}$$

Here (r,ϕ) are polar coordinates centered at O and $\mathbf{e}_r$, $\mathbf{e}_\phi$ are the corresponding unit vectors.

The second step is the up scaling step. Here one solves (1.7) in the unit cell containing the Hashin–Shtrikman-coated cylinder assemblage. In the context of anti-plane shear (1.7) reduces to

$$-\mathrm{div}_{\mathbf{y}}(2G(\mathbf{y})(\nabla_{\mathbf{y}}(w(\mathbf{x},\mathbf{y})) + \nabla u^{\mathrm{M}}(\mathbf{x}))) = 0, \quad \mathbf{y}\ \text{in}\ Q, \tag{2.5}$$

where $G(\mathbf{y})$ is the piecewise constant shear modulus in the coated cylinder assemblage taking the values G_{m} in the matrix and G_{f} in the fibers. For $\mathbf{x}$ fixed $\nabla u^{\mathrm{M}}(\mathbf{x})$ is a constant vector and the fields $w(\mathbf{x},\mathbf{y})$ and $\sigma(\mathbf{x},\mathbf{y}) = 2G(\mathbf{y})(\nabla_{\mathbf{y}}(w(\mathbf{x},\mathbf{y})) + \nabla u^{\mathrm{M}}(\mathbf{x}))$ can be solved analytically, see Hashin and Shtrikman (1962). Here, the macrostress modulation in the matrix and fiber phases are given by

$$f^{\mathrm{m}}(\mathbf{x}) = \||\sigma(\mathbf{x},\mathbf{y})|\|_{L^\infty(Q_{\mathrm{m}})} \tag{2.6}$$

and

$$f^{\mathrm{f}}(\mathbf{x}) = \||\sigma(\mathbf{x},\mathbf{y})|\|_{L^\infty(Q_{\mathrm{f}})}; \tag{2.7}$$

respectively, where Q_{m} is the part of the unit cell occupied by matrix and Q_{f} is the part occupied by fibers. Changing to polar coordinates and solution of (2.5) gives

$$f^{\mathrm{m}}(r,\phi) = K^{\mathrm{m}}\frac{\pi}{\omega}r^{\pi/\omega-1} \tag{2.8}$$

and

$$f^{\mathrm{f}}(r,\phi) = K^{\mathrm{f}}\frac{\pi}{\omega}\, r^{\pi/\omega-1}, \tag{2.9}$$

where

$$K^{\mathrm{m}} = \frac{1+|\beta-\alpha|/(\beta+\alpha)}{1-\theta(\beta-\alpha)/(\beta+\alpha)} \tag{2.10}$$

and

$$K^{\mathrm{f}} = \frac{2\alpha}{\beta+\alpha-\theta(\beta-\alpha)}. \tag{2.11}$$

Formulas (2.10) and (2.11) imply that $1 \leqslant K^{\mathrm{f}} \leqslant K^{\mathrm{m}}$. When the fiber is stiffer than the matrix $K^{\mathrm{f}} = K^{\mathrm{m}}$ and when the fiber is more compliant then $K^{\mathrm{f}} < K^{\mathrm{m}}$. Thus it is clear that

$$M(r,\phi) = \max\{f^{\mathrm{m}}(r,\phi), f^{\mathrm{f}}(r,\phi)\} = f^{\mathrm{m}}(r,\phi). \tag{2.12}$$

The area of the cross section with reentrant corner is denoted by A and for the case considered here $A = \omega/2$. The calculation gives

$$|\{f^{\mathrm{m}}(r,\phi) \geqslant t\}| = A\left(K^{\mathrm{m}}\frac{\pi}{\omega}\right)^{2\omega/(\omega-\pi)} \times t^{-2\omega/(\omega-\pi)} \quad \text{for } t > K^{\mathrm{m}}\frac{\pi}{\omega} \tag{2.13}$$

and

$$|\{f^{\mathrm{f}}(r,\phi) \geqslant t\}| = A\left(K^{\mathrm{f}}\frac{\pi}{\omega}\right)^{2\omega/(\omega-\pi)} \times t^{-2\omega/(\omega-\pi)} \quad \text{for } t > K^{\mathrm{f}}\frac{\pi}{\omega} \tag{2.14}$$

and $|\{f^{\mathrm{m}}(r,\phi) \geqslant t\}| = A$ for $t \leqslant K^{\mathrm{m}}\frac{\pi}{\omega}$ and $|\{f^{\mathrm{f}}(r,\phi) \geqslant t\}| = A$ for $t \leqslant K^{\mathrm{f}}\frac{\pi}{\omega}$. Proposition 1.1 immediately gives the bounds

$$\lim_{\varepsilon_k\to 0}\lambda_{\mathrm{m}}^{\varepsilon_k}(t) \leqslant \begin{cases} A\left(K^{\mathrm{m}}\dfrac{\pi}{\omega}\right)^{2\omega/(\omega-\pi)} \times t^{-2\omega/(\omega-\pi)} & \text{for } t > K^{\mathrm{m}}\dfrac{\pi}{\omega}, \\ A & \text{for } t \leqslant K^{\mathrm{m}}\dfrac{\pi}{\omega} \end{cases} \tag{2.15}$$

and

$$\lim_{\varepsilon_k\to 0}\lambda_{\mathrm{f}}^{\varepsilon_k}(t) \leqslant \begin{cases} A\left(K^{\mathrm{f}}\dfrac{\pi}{\omega}\right)^{2\omega/(\omega-\pi)} \times t^{-2\omega/(\omega-\pi)} & \text{for } t > K^{\mathrm{f}}\dfrac{\pi}{\omega}, \\ A & \text{for } t \leqslant K^{\mathrm{f}}\dfrac{\pi}{\omega}. \end{cases} \tag{2.16}$$

For comparison it is noted that the stress distribution $\lambda_{\mathrm{m}}(t)$ inside the cross section filled with pure matrix material and no fibers is given by

$$\lambda_{\mathrm{m}}(t) = \begin{cases} A\left(\dfrac{\pi}{\omega}\right)^{2\omega/(\omega-\pi)} \times t^{-2\omega/(\omega-\pi)} & \text{for } t > \dfrac{\pi}{\omega}, \\ A & \text{for } t \leqslant \dfrac{\pi}{\omega}. \end{cases} \tag{2.17}$$

It is noted that $K^{\mathrm{m}} = 1$ when $G_{\mathrm{f}} = G_{\mathrm{m}}$ and one sees that the upper bound (2.15) coincides with the exact result (2.17) in the absence of reinforcement. In Section 3, we identify generic situations for which the volume of the overstressed zones have polynomial decay of the kind given by (2.15) and (2.16).

Next we apply Propositions 1.3 and 1.4 to identify the location and extent of the overstressed zone due to the stress concentration at the reentrant corner. For a prescribed value of t the radii $d_{\mathrm{m}} = d_{\mathrm{m}}(t)$ and $d_{\mathrm{f}} = d_{\mathrm{f}}(t)$ are defined by

$$f^{\mathrm{m}}(d_{\mathrm{m}}, \phi) = K^{\mathrm{m}} \frac{\pi}{\omega} d_{\mathrm{m}}^{\pi/\omega - 1} = t \tag{2.18}$$

and

$$f^{\mathrm{f}}(d_{\mathrm{f}}, \phi) = K^{\mathrm{f}} \frac{\pi}{\omega} d_{\mathrm{f}}^{\pi/\omega - 1} = t. \tag{2.19}$$

From Proposition 1.3 it follows that for any set S containing only points with radial coordinate $r > d_{\mathrm{f}}$ that

$$\lim_{\varepsilon_k \to 0} \lambda_{\mathrm{f}}^{\varepsilon_k}(t, S) = 0, \tag{2.20}$$

and for any set S containing only points with radial coordinate $r > d_{\mathrm{m}}$ that

$$\lim_{\varepsilon_k \to 0} \lambda_{\mathrm{m}}^{\varepsilon_k}(t, S) = 0. \tag{2.21}$$

From Proposition 1.4 and (2.12) it follows that for sets S containing only points with radial coordinate $r > d_{\mathrm{m}}$ that

$$\lim_{\varepsilon_k \to 0} \lambda^{\varepsilon_k}(t, S) = 0. \tag{2.22}$$

For small values of ε_k, it is clear from (2.20), (2.21), and (2.22) that the radii $d_{\mathrm{m}}(t)$ and $d_{\mathrm{f}}(t)$ provide estimates for the extension of the overstressed regions $S_{\mathrm{m},t}^{\varepsilon_k}$, $S_t^{\varepsilon_k}$, and $S_{\mathrm{f},t}^{\varepsilon_k}$ inside the composite. It is evident from their definition that d_{m} and d_{f} depend explicitly on the volume fraction of fibers in the microstructure. To illustrate the ideas it is supposed that the fiber shear modulus is 1 the matrix shear modulus is 20 and the area fraction of fibers is taken to be 0.6. For these values $K^{\mathrm{m}} = 7.14$. In Fig. 4, the radius $d_{\mathrm{m}}(7) = 0.296$ is plotted for a domain with $\omega = 3\pi/2$. It is evident from (2.20), (2.21), and (2.22) that progressively larger portions of the overstressed regions $S_{\mathrm{m},7}^{\varepsilon_k}$, $S_7^{\varepsilon_k}$, and $S_{\mathrm{f},7}^{\varepsilon_k}$ lie within the radius 0.296 as ε_k tends to zero. Indeed, there is a length scale ε_k for which more than 99.9% of the areas of the sets $S_{\mathrm{m},7}^{\varepsilon_k}$, $S_7^{\varepsilon_k}$, and $S_{\mathrm{f},7}^{\varepsilon_k}$ lie inside the radius 0.296.

Next we consider a shaft cross section given by a half disk of radius 0.3. The flat part of the half disk lies on the x_1-axis and the origin for the x_1, x_2 coordinate system lies midway between the ends. The disk contains periodic microgeometry with period cells filled with the Hashin–Shtrikman-coated sphere assemblage and is subjected to an anti-plane shear load. On $-0.3 < x_1 < 0$ we prescribe the traction boundary condition $\sigma^{\varepsilon^k} \cdot \mathbf{n} = \pi$, on $0 < x_1 < 0.3$ we prescribe $\sigma^{\varepsilon^k} \cdot \mathbf{n} = 0$ and on the circular

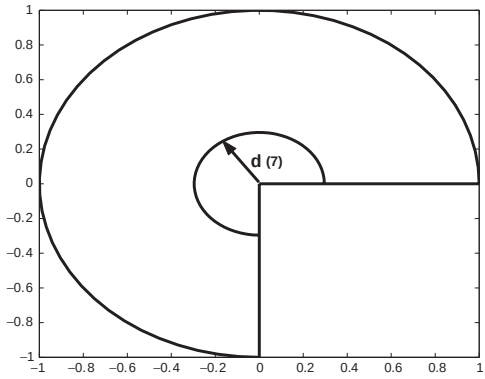

Fig. 4. Rigorous estimation of the overstressed zone for the reentrant corner in a fiber-reinforced composite shaft subject to anti-plane shear.

arc $r = 0.3,\ 0 < \phi < \pi$ the traction is given by $\sigma^{\varepsilon^k} \cdot \mathbf{n} = (\ln 0.3 + 1)\cos\phi - \phi \sin\phi$. Proceeding as before we find that

$$f^{\mathrm{m}}(r,\phi) = K^{\mathrm{m}}\sqrt{(\ln r + 1)^2 + \phi^2} \tag{2.23}$$

and

$$f^{\mathrm{f}}(r,\phi) = K^{\mathrm{f}}\sqrt{(\ln r + 1)^2 + \phi^2}. \tag{2.24}$$

Application of Propositions 1.1 and 1.2 shows that

$$\lim_{\varepsilon_k \to 0} \lambda_{\mathrm{m}}^{\varepsilon_k}(t) \leqslant \left|\left\{K^{\mathrm{m}}\sqrt{(\ln r + 1)^2 + \phi^2} \geqslant t\right\}\right|, \tag{2.25}$$

$$\lim_{\varepsilon_k \to 0} \lambda_{\mathrm{f}}^{\varepsilon_k}(t) \leqslant \left|\left\{K^{\mathrm{f}}\sqrt{(\ln r + 1)^2 + \phi^2} \geqslant t\right\}\right| \tag{2.26}$$

and

$$\lim_{\varepsilon_k \to 0} \lambda^{\varepsilon_k}(t) \leqslant \left|\left\{K^{\mathrm{m}}\sqrt{(\ln r + 1)^2 + \phi^2} \geqslant t\right\}\right|. \tag{2.27}$$

The fiber area fraction and fiber and matrix shear moduli are chosen as before to be $G_{\mathrm{m}} = 20$, $G_{\mathrm{f}} = 1$, and $\theta = 0.6$. For this choice $K^{\mathrm{m}} = 7.14$. We choose $t = 22.25$ and the set specified by

$$\left\{(r,\phi); 7.14\sqrt{(\ln r + 1)^2 + \phi^2} \geqslant 22.5\right\} \tag{2.28}$$

is given by the shaded region inside the half disk shown in Fig. 5. From Proposition 1.4 it follows that for any set S that does not intersect the shaded region that

$$\lim_{\varepsilon_k \to 0} \lambda^{\varepsilon_k}(22.5, S) = 0. \tag{2.29}$$

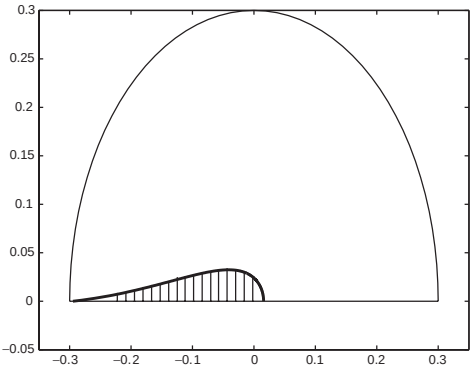

Fig. 5. The shaded region gives a rigorous estimation for the overstressed zone due to a change in traction on the boundary of a fiber-reinforced composite shaft subject to anti-plane shear.

Thus for microstructure characterized by sufficiently small ε_k, the shaded region gives an estimate for the overstressed region $S^{\varepsilon_k}_{\mathrm{m},22.5}$. The shaded region provides a rigorous upper bound on the over stressed region in the sense of (2.29) in the $\varepsilon_k = 0$ limit. It is noted that for sufficiently large values of t and sufficiently small values of r the volume $\left|\left\{K^{\mathrm{m}}\sqrt{(\ln r+1)^2+\phi^2} \geqslant t\right\}\right|$ is well approximated by $(\pi/2)e^2\exp(-t/K^{\mathrm{m}})$. In Section 3, we identify generic situations under which the volume of the overstressed zones have exponential decay.

Last consider an L-shaped cross section subject to torsional loading. The cross section is filled with a ε_k periodic repetition of the Hashin–Shtrikman-coated cylinder assemblage. The stress potential φ^{ε_k} vanishes on the boundary of the cross section and satisfies

$$-\Delta\varphi^{\varepsilon_k} = 2G_{\mathrm{m}} \text{ in the matrix}$$

and

$$-\Delta\varphi^{\varepsilon_k} = 2G_{\mathrm{f}} \text{ in the fibers.} \tag{2.30}$$

The stress potential is continuous across material interfaces and

$$(2G_{\mathrm{m}})^{-1}\partial_{\mathrm{n}}\varphi^{\varepsilon_k}_{\mathrm{m}} = (2G_{\mathrm{f}})^{-1}\partial_{\mathrm{n}}\varphi^{\varepsilon_k}_{\mathrm{f}}. \tag{2.31}$$

Proceeding with the multi-scale analysis we first write the associated homogenized boundary value problem for the macroscopic stress potential φ^{M} obtained in the $\varepsilon_k = 0$ limit. Here $\varphi^{\mathrm{M}} = 0$ on the boundary of the L-shaped domain and

$$-h^{\mathrm{E}}\Delta\varphi^{\mathrm{M}} = 1, \tag{2.32}$$

where

$$h^{\mathrm{E}} = \beta\left(\frac{\beta(1-\theta)+\alpha(1+\theta)}{\beta(1+\theta)+\alpha(1-\theta)}\right). \tag{2.33}$$

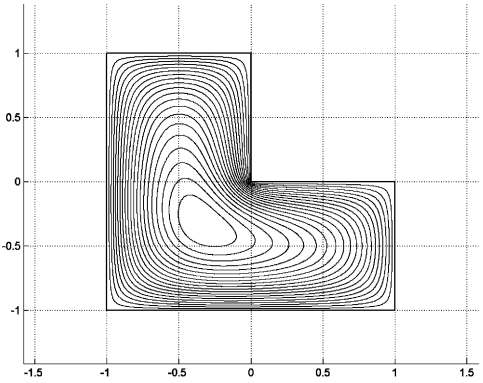

Fig. 6. Contour plot of macroscopic stress potential.

Here $\beta = (2G_{\mathrm{m}})^{-1}$, $\alpha = (2G_{\mathrm{f}})^{-1}$ and θ is the area fraction of the fiber phase. The macroscopic stress potential is solved numerically and is plotted in Fig. 6. Next we up scale and solve for the macrostress modulation functions. For this example, the up-scaling step requires us to solve for the fluctuating stress potential $w(\mathbf{y},\mathbf{x})$. Here w is Q periodic in the $\mathbf{y}$ variable and is the solution of

$$-\operatorname{div}_{\mathbf{y}}((2G(\mathbf{y}))^{-1}(\nabla_{\mathbf{y}}(w(\mathbf{x},\mathbf{y})) + \nabla\varphi^{\mathrm{M}}(\mathbf{x}))) = 0, \quad \mathbf{y} \text{ in } Q, \tag{2.34}$$

where $G(\mathbf{y})$ is the piecewise constant shear modulus in the coated cylinder assemblage taking the values G_{m} in the matrix and G_{f} in the fibers. For $\mathbf{x}$ fixed $\nabla\varphi^{\mathrm{M}}(\mathbf{x})$ is a constant vector and the field $w(\mathbf{x},\mathbf{y})$ can be solved analytically. For this problem the macrostress modulation functions are written in the form

$$f^{\mathrm{m}}(\mathbf{x}) = \||\nabla_{\mathbf{y}} w(\mathbf{x},\mathbf{y}) + \nabla\varphi^{\mathrm{M}}(\mathbf{x})|\|_{L^\infty(Q_{\mathrm{m}})} \tag{2.35}$$

and

$$f^{\mathrm{f}}(\mathbf{x}) = \||\nabla_{\mathbf{y}} w(\mathbf{x},\mathbf{y}) + \nabla\varphi^{\mathrm{M}}(\mathbf{x})|\|_{L^\infty(Q_{\mathrm{f}})}. \tag{2.36}$$

see Lipton (2003). Solution of (2.34) gives

$$f^{\mathrm{m}}(\mathbf{x}) = \tilde{K}^{\mathrm{m}}|\nabla\varphi^{\mathrm{M}}(\mathbf{x})| \tag{2.37}$$

and

$$f^{\mathrm{f}}(\mathbf{x}) = \tilde{K}^{\mathrm{f}}|\nabla\varphi^{\mathrm{M}}(\mathbf{x})|. \tag{2.38}$$

Here,

$$\tilde{K}^{\mathrm{m}} = \frac{1 + |\beta - \alpha|/(\beta + \alpha)}{1 + \theta(\beta - \alpha)/(\beta + \alpha)} \tag{2.39}$$

and

$$\tilde{K}^{\mathrm{f}} = \frac{2\beta}{\beta + \alpha + \theta(\beta - \alpha)}. \tag{2.40}$$

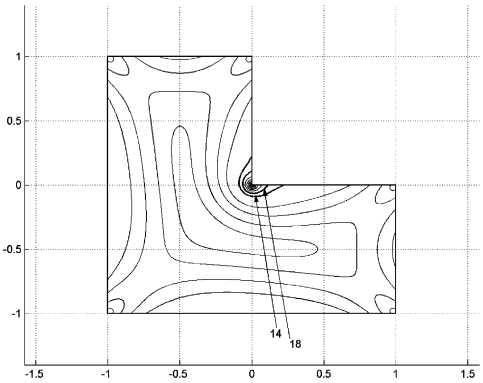

Fig. 7. Rigorous estimation of the overstressed zone for a fiber-reinforced composite shaft with L-shaped cross section subject to torsion loading.

To illustrate the ideas, we choose $G_{\rm m}=10$, $G_{\rm f}=1$ and $\theta=0.2$. For these choices $h^{\rm E}=0.7$, $\tilde{K}^{\rm m}=2.174$ and $\tilde{K}^{\rm f}=0.2174$. The level curves for $f^{\rm m}(\mathbf{x})$ are plotted in Fig. 7. The level curve $\{f^{\rm m}(\mathbf{x})=14\}$ is highlighted in Fig. 7. The set of points surrounded by the curve and the reentrant corner is precisely the set $\{f^{\rm m}(\mathbf{x})\geqslant 14\}$. The set of points outside this zone is precisely the set $\{f^{\rm m}(\mathbf{x})<14\}$. It is evident from Proposition 1.3 that $\lim_{\varepsilon_k\to 0}\lambda_{\rm m}^{\varepsilon_k}(14,S)=0$ for any set S contained within $\{f^{\rm m}(\mathbf{x})<14\}$. In this way we see that the set $\{f^{\rm m}(\mathbf{x})\geqslant 14\}$ provides a good estimate for the overstressed zone $\{|\nabla\varphi^{\varepsilon_k}|>14\}$ when ε_k is sufficiently small.

3. Bounds with exponential and polynomial decay: sufficient conditions

Motivated by the examples given in the previous section we identify generic conditions under which the bounds on $\lim_{\varepsilon_k\to 0}\lambda_i^{\varepsilon_k}(t)$ exhibit polynomial or exponential decay. The results presented here easily follow from Propositions 1.1 and 1.2 given in the introduction. The utility of these results lies in the fact that they apply to composites made from of N anisotropic elastic materials and they apply to samples with reentrant corners.

In the first example of Section 2 bounds on $\lim_{\varepsilon_k\to 0}\lambda_i^{\varepsilon_k}(t)$ were found that exhibited polynomial decay in t. Motivated by this example we give general conditions for which $\lim_{\varepsilon_k\to 0}\lambda_i^{\varepsilon_k}(t)\leqslant Kt^{-p}$. Such a bound follows immediately from Proposition 1.1 when it is known that for some p with $1\leqslant p<\infty$ that

$$\|f^i(\mathbf{S}^{\rm E}\sigma^{\rm M}(\mathbf{x}))\|_{L^p}^p=\int_\Omega (f^i(\mathbf{S}^{\rm E}\sigma^{\rm M}(\mathbf{x})))^p\,{\rm d}\mathbf{x}<\infty. \tag{3.1}$$

For this case one has the bound given by

Proposition 3.1.

$$\lim_{\varepsilon_k\to 0}\lambda_i^{\varepsilon_k}(t)\leqslant \|f^i(\mathbf{S}^{\rm E}\sigma^{\rm M}(\mathbf{x}))\|_{L^p}^p\times t^{-p}. \tag{3.2}$$

In the second example of Section 2 bounds on $\lim_{\varepsilon_k\to 0}\lambda^{\varepsilon_k}(t)$ are found that decay exponentially. The macrostress modulation function for this example behaved asymptotically like $K^{\mathrm{m}}|\ln r|$ in the limit as $r\to 0$. Although $|\ln r|$ is unbounded it does have bounded mean oscillation (BMO). Motivated by this example, we consider an open cube C_0 immersed inside the composite and give general conditions for which the upper bound on $\lim_{\varepsilon_k\to 0}\lambda^{\varepsilon_k}(t,C_0)$ decays exponentially in t. We recall the macro stress modulation $M(\mathbf{S}^{\mathrm{E}}\sigma^{\mathrm{M}}(\mathbf{x}))$ given by

$$M(\mathbf{S}^{\mathrm{E}}\sigma^{\mathrm{M}}(\mathbf{x})) = \max_{i=1,\ldots,N} f^i(\mathbf{S}^{\mathrm{E}}\sigma^{\mathrm{M}}(\mathbf{x})). \tag{3.3}$$

The BMO norm of $M(\mathbf{S}^{\mathrm{E}}\sigma^{\mathrm{M}}(\mathbf{x}))$ over the cube C_0 is given by

$$\|M\|_{\mathrm{BMO}} = \sup_{C\subset C_0}\left(\frac{1}{|C|}\int_C |M(\mathbf{S}^{\mathrm{E}}\sigma^{\mathrm{M}}(\mathbf{x})) - M_C|\,\mathrm{d}\mathbf{x}\right), \tag{3.4}$$

where M_C is the average of $M(\mathbf{S}^{\mathrm{E}}\sigma^{\mathrm{M}}(\mathbf{x}))$ over C and the supremum is taken over all sub-cubes C of C_0. The BMO norm and the space of functions of bounded mean oscillation were introduced by John and Nirenberg (1961).

For any positive number α between zero and one we define the constant $C(\alpha)$ by

$$C(\alpha) = \frac{\alpha|\ln\alpha|}{8\|M\|_{\mathrm{BMO}}}. \tag{3.5}$$

Next we denote the average of $M(\mathbf{S}^{\mathrm{E}}\sigma^{\mathrm{M}}(\mathbf{x}))$ over the cube C_0 by M_{C_0} and the bound on $\lim_{\varepsilon_k\to 0}\lambda^{\varepsilon_k}(t,C_0)$ is given in the following proposition.

Proposition 3.2. *If* $t > 8\|M\|_{\mathrm{BMO}}\alpha^{-1} + M_{C_0}$ *then*

$$\lim_{\varepsilon_k\to 0}\lambda^{\varepsilon_k}(t,C_0) \leqslant \alpha^{-1}\mathrm{e}^{-C(\alpha)\times(t-M_{C_0})}. \tag{3.6}$$

For t fixed the Proposition shows that $\lambda^{\varepsilon_k}(t,C_0)$ approaches or drops below

$$\alpha^{-1}\mathrm{e}^{-C(\alpha)\times(t-M_{C_0})}$$

for ε_k sufficiently small. It also shows that the upper bound is exponentially decreasing for large t. Optimization over α, see Section 5, provides the tighter upper bound given by the following Proposition.

Proposition 3.3. *If* $t > 8\|M\|_{\mathrm{BMO}} + M_{C_0}$ *then*

$$\lim_{\varepsilon_k\to 0}\lambda^{\varepsilon_k}(t,C_0) \leqslant (\alpha(t))^{-1}e\times \mathrm{e}^{[-\alpha(t)(t-M_{C_0})/(8\|M\|_{\mathrm{BMO}})]}, \tag{3.7}$$

where the factor $\alpha(t)$ *lies in the interval* $e^{-1} < \alpha(t) < 1$ *and is the root of the equation*

$$\kappa^{-1} - \alpha(1+\ln\alpha) = 0, \tag{3.8}$$

with $\kappa = (t - M_{C_0})/(8\|M\|_{\mathrm{BMO}})$.

4. Derivation of basic inequalities

In this section we derive Propositions 1.1 and 1.2. These are shown to follow in a straight forward manner from the homogenization constraint given in Lipton (2003).

In order to introduce the constraint we define the distribution of states for the equivalent stress in a composite. Recall that the set in the ith phase where the equivalent stress exceeds t is denoted by $S^{\varepsilon_k}_{t,i}$. Consider any subset S of the specimen. The distribution function $\lambda^{\varepsilon_k}_i(t,S)$ is defined by $\lambda^{\varepsilon_k}_i(t,S)=|S^{\varepsilon_k}_{t,i}\cap S|$. The indicator function for the set $S^{\varepsilon_k}_{t,i}$ is written $\chi^{\varepsilon_k}_{t,i}$ taking the value 1 in $S^{\varepsilon_k}_{t,i}$ and 0 outside and we write $\lambda^{\varepsilon_k}_i(t,S)=\int_S \chi^{\varepsilon_k}_{t,i}\,\mathrm{d}\mathbf{x}$. From the theory of weak convergence (see Evans, 1990) there exists a density $\theta_{t,i}(\mathbf{x})$ taking values in the interval [0,1] such that (on passage to a subsequence if necessary) for every choice of S one has $\lim_{k\to\infty}\lambda^{\varepsilon_k}_i(t,S)=\int_S\theta_{t,i}(\mathbf{x})\,\mathrm{d}x$. The density $\theta_{t,i}(\mathbf{x})$ is the local distribution of states of the equivalent stress $\sigma^{\varepsilon_k}_{\mathrm{eq}}$ in the limit of vanishing ε_k. One also considers the indicator function $\chi^{\varepsilon_k}_t$ for the set $S^{\varepsilon_k}_t$ where the equivalent stress is greater than t. Its clear that this set is the union of the sets $S^{\varepsilon_k}_{t,i}$. As before there is a density $\theta_t(\mathbf{x})$ such that $\lim_{k\to\infty}\lambda^{\varepsilon_k}(t,S)=\int_S\theta_t(\mathbf{x})\,\mathrm{d}x$, for every choice of set S. It follows easily that $\sum_i\theta_{t,i}=\theta_t$, where $0\leqslant\theta_t\leqslant 1$.

An application of Theorem 4.2 of Lipton (2003) delivers the homogenization constraints

$$\theta_{t,i}(\mathbf{x})(f^i(\mathbf{S}^{\mathrm{E}}\sigma^{\mathrm{M}}(\mathbf{x}))-t)\geqslant 0,\quad i=1,\ldots,N. \tag{4.1}$$

We now prove a slight generalization of Proposition 1.1. It is evident from Eq. (4.1) that at (almost) every point for which $\theta_{t,i}(\mathbf{x})>0$ one has that $f^i(\mathbf{S}^{\mathrm{E}}\sigma^{\mathrm{M}}(\mathbf{x}))\geqslant t$. Now consider a subset S of the composite domain. The set of points in S for which $\theta_{t,i}(\mathbf{x})>0$ is denoted by $\{\mathbf{x}\text{ in }S;\theta_{t,i}(\mathbf{x})>0\}$ and it is clear that

$$|\{\mathbf{x}\text{ in }S;\theta_{t,i}(\mathbf{x})>0\}|\leqslant|\{\mathbf{x}\text{ in }S;f^i(\mathbf{S}^{\mathrm{E}}\sigma^{\mathrm{M}}(\mathbf{x}))\geqslant t\}|. \tag{4.2}$$

Since $0\leqslant\theta_{t,i}(\mathbf{x})\leqslant 1$ one has the estimate

$$\lim_{k\to\infty}\lambda^{\varepsilon_k}_i(t,S)=\int_S\theta_{t,i}(\mathbf{x})\,\mathrm{d}\mathbf{x}\leqslant|\{\mathbf{x}\text{ in }S;\theta_{t,i}(\mathbf{x})>0\}| \tag{4.3}$$

and from (4.2) we deduce that

$$\lim_{k\to\infty}\lambda^{\varepsilon_k}_i(t,S)\leqslant|\{\mathbf{x}\text{ in }S;f^i(\mathbf{S}^{\mathrm{E}}\sigma^{\mathrm{M}}(\mathbf{x}))\geqslant t\}|. \tag{4.4}$$

Proposition 1.1 follows on making the choice $S=\Omega$ in (4.4).

Adding the homogenization constraints (4.1) and noting that $M(\mathbf{S}^{\mathrm{E}}\sigma^{\mathrm{M}}(\mathbf{x}))\geqslant f^i(\mathbf{S}^{\mathrm{E}}\sigma^{\mathrm{M}}(\mathbf{x}))$ and $\sum_i\theta_{t,i}(\mathbf{x})=\theta_t(\mathbf{x})\leqslant 1$ we have

$$\theta_t(\mathbf{x})(M(\mathbf{S}^{\mathrm{E}}\sigma^{\mathrm{M}}(\mathbf{x}))-t)\geqslant 0,\quad i=1,\ldots,N. \tag{4.5}$$

Arguing as before we find that

$$\lim_{k\to\infty}\lambda^{\varepsilon_k}(t,S)\leqslant|\{\mathbf{x}\text{ in }S;M(\mathbf{S}^{\mathrm{E}}\sigma^{\mathrm{M}}(\mathbf{x}))\geqslant t\}|. \tag{4.6}$$

Proposition 1.2 follows on making the choice $S=\Omega$ in (4.6).

5. Derivation of the sufficient conditions for polynomial and exponential decay

In this section, Propositions 3.1–3.3 are derived. To prove Proposition 3.1, we apply a basic estimate for the right-hand side of Eq. (4.4) when it is known that $\|f^i(\mathbf{S}^{\mathrm{E}}\sigma^{\mathrm{M}}(\mathbf{x}))\|_{L^p} \leqslant \infty$. The estimate is given by

$$|\{\mathbf{x} \text{ in } S; f^i(\mathbf{S}^{\mathrm{E}}\sigma^{\mathrm{M}}(\mathbf{x})) \geqslant t\}| \leqslant \|f^i(\mathbf{S}^{\mathrm{E}}\sigma^{\mathrm{M}}(\mathbf{x}))\|^p_{L^p} \times t^{-p} \tag{5.1}$$

and Proposition 3.1 follows.

Now, we derive Propositions 3.2 and 3.3. We apply the John–Nirenberg Theorem (1961) to estimate the right-hand side of (4.6) with $S = C_0$. To do this, we show first that

$$\begin{aligned}|\{\mathbf{x} \text{ in } C_0; M(\mathbf{S}^{\mathrm{E}}\sigma^{\mathrm{M}}(\mathbf{x})) \geqslant t\}| \leqslant |\{\mathbf{x} \text{ in } C_0; |M(\mathbf{S}^{\mathrm{E}}\sigma^{\mathrm{M}}(\mathbf{x})) - M_{C_0}| \\ \geqslant t - M_{C_0}\}|.\end{aligned} \tag{5.2}$$

To see this note that since $M(\mathbf{S}^{\mathrm{E}}\sigma^{\mathrm{M}}(\mathbf{x}))$ is non-negative one has that $M(\mathbf{S}^{\mathrm{E}}\sigma^{\mathrm{M}}(\mathbf{x})) \leqslant |M(\mathbf{S}^{\mathrm{E}}\sigma^{\mathrm{M}}(\mathbf{x})) - M_{C_0}| + M_{C_0}$. Thus,

$$\{\mathbf{x} \text{ in } C_0; M(\mathbf{S}^{\mathrm{E}}\sigma^{\mathrm{M}}(\mathbf{x})) \geqslant t\} \subset \{\mathbf{x} \text{ in } C_0; |M(\mathbf{S}^{\mathrm{E}}\sigma^{\mathrm{M}}(\mathbf{x})) - M_{C_0}| \geqslant t - M_{C_0}\} \tag{5.3}$$

and (5.2) follows. Application of the John–Nirenberg Theorem (1961) gives

$$\begin{aligned}&\frac{|\{\mathbf{x} \text{ in } C_0; |M(\mathbf{S}^{\mathrm{E}}\sigma^{\mathrm{M}}(\mathbf{x})) - M_{C_0}| \geqslant s\}|}{|C_0|} \\ &\leqslant \begin{cases} 1, & \text{for } 0 < s \leqslant 8\|M\|_{\mathrm{BMO}}\alpha^{-1}, \\ \alpha^{-1}\mathrm{e}^{[-(C(\alpha)\times(s)]}, & \text{for } 8\|M\|_{\mathrm{BMO}}\alpha^{-1} < s. \end{cases}\end{aligned} \tag{5.4}$$

Proposition 3.2 follows immediately from the change of variables $s = t - M_{C_0}$ and inequalities (4.6), (5.2), and (5.4). The function obtained by the change of variables $s = t - M_{C_0}$ in Eq. (5.4) is denoted by $\bar{P}_\alpha(t, C_0)$ and

$$\bar{P}_\alpha(t, C_0) = \begin{cases} 1, & \text{for } 0 < t - M_{C_0} \leqslant 8\|M\|_{\mathrm{BMO}}\alpha^{-1}, \\ \alpha^{-1}\mathrm{e}^{[-(C(\alpha)\times(t-M_{C_0})]}, & \text{for } 8\|M\|_{\mathrm{BMO}}\alpha^{-1} < t - M_{C_0}. \end{cases} \tag{5.5}$$

It is evident from the estimates that $\lim_{\varepsilon_k\to 0}\lambda^{\varepsilon_k}(t, C_0) \leqslant \bar{P}_\alpha(t, C_0)$, for $M_{C_0} < t$. Tighter upper bounds are given by optimizing over α, i.e.,

$$\lim_{\varepsilon_k\to 0}\lambda^{\varepsilon_k}(t, C_0) \leqslant \bar{U}(t, C_0) = \inf_{0<\alpha<1}\bar{P}_\alpha(t, C_0). \tag{5.6}$$

Here $\bar{U}(t, C_0)$ is continuous and decreasing and is given by

$$\bar{U}(t, C_0) = \begin{cases} 1 & \text{for } 0 < t - M_{C_0} \leqslant 8\|M\|_{\mathrm{BMO}}, \\ (\alpha(t))^{-1}e \times \mathrm{e}^{[-\alpha(t)(t-M_{C_0})/(8\|M\|_{\mathrm{BMO}})]}, & \text{for } 8\|M\|_{\mathrm{BMO}} + M_{C_0} < t. \end{cases} \tag{5.7}$$

The factor $\alpha(t)$ lies in the interval $e^{-1} < \alpha(t) < 1$ and is the root of the equation

$$\kappa^{-1} - \alpha(1 + \ln \alpha) = 0, \tag{5.8}$$

where $\kappa = (t - M_{C_0})/(8\|M\|_{\mathrm{BMO}})$. Proposition 3.3 now follows immediately from (5.7).

Acknowledgements

This research effort is sponsored by NSF through grant DMS-0296064 and by the Air Force Office of Scientific Research, Air Force Material Command USAF, under grant number F49620-02-1-0041. The US Government is authorized to reproduce and distribute reprints for governmental purposes notwithstanding any copyright notation thereon. The views and conclusions herein are those of the authors and should not be interpreted as necessarily representing the official policies or endorsements, either expressed or implied of the Air Force Office of Scientific Research or the US Government.

References

Bensoussan, A., Lions, J.L., Papanicolaou, G., 1978. Asymptotic Analysis for Periodic Structures. In: Studies in Mathematics and its Applications, Vol. 5. North-Holland, Amsterdam.

Evans, L.C., 1990. Weak Convergence Methods for Nonlinear Partial Differential Equations. CBMS Regional Conference Series in Mathematics, No. 74. American Mathematical Society, Providence, RI.

Hashin, Z., Shtrikman, S., 1962. A variational approach to the theory of the effective magnetic permeability of multiphase materials. J. Appl. Phys. 33, 3125–3131.

Jeulin, D., 1994. Random structure models for composite media and fracture statistics. In: Markov, K.Z. (Ed.), Advances in Mathematical Modeling of Composite Materials, Advances in Mathematics for Applied Sciences, Vol. 15. World Scientific Company, Singapore, pp. 239–289.

John, F., Nirenberg, L., 1961. On functions of bounded mean oscillation. Comm. Pure Appl. Math. 14, 415–426.

Kelly, A., Macmillan, N.H., 1986. Strong solids. Monographs on the Physics and Chemistry of Materials. Clarendon Press, Oxford.

Lipton, R., 2003. Assessment of the local stress state through macroscopic variables. Philos. Trans. Roy. Soc. Math. Phy. Eng. Sc. 361, 921–946.

Luciano, R., Willis, J.R., 2003. Boundary–layer corrections for stress and strain fields in randomly heterogeneous materials. J. Mech. Phys. Solids 51, 1075–1088.

Milton, G.W., 2002. The theory of composites. In: Applied and Computational Mathematics, Vol. 6. Cambridge University Press, Cambridge.

Tsai, S.W., Hahn, H.T., 1980. Introduction to Composite Materials. Technomic Press, Lancaster, PA.